Product Branching Ratios of the CH + NO Reaction

A. Bergeat, T. Calvo, N. Daugey, J.-C. Loison, and G. Dorthe*

Laboratoire de Physico-Chimie Moléculaire, CNRS UMR 5803, Université Bordeaux I, F-33405 Talence Cedex, France

Received: May 1, 1998; In Final Form: August 3, 1998

The multichannel CH + NO reaction was studied, at room temperature, in a low-pressure fast-flow reactor. CH was obtained from the reaction of $CHBr_3$ with potassium atoms. The overall rate constant was found to be $(1.9 \pm 0.5) \times 10^{-10}$ cm^3 molecule^{-1} s^{-1}. The relative branching ratios of NH($A^3\Pi$) + CO and NCO($A^2\Sigma^+$) + H chemiluminescent pathways were determined as 42% and 58% (±7). Nascent NH($A^3\Pi$) was distributed between the vibrational levels $v' = 1$ and $v' = 0$ in the proportion of 33% and 67% (±3%). The CN chemiluminescence from the energetically allowed CN($A^2\Pi_i$) + OH pathway could not be detected. Also, CN($X^2\Sigma^+$) could not be detected by laser-induced fluorescence. Relative product branching ratios were determined over the channels yielding atoms probed by resonance fluorescence in the vacuum ultraviolet: O + HCN, (72 ± 10)%; H + NCO, (21 ± 10)%; N + HCO, (7 ± 3)%.

I. Introduction

The CH + NO reaction is known to play an important role in combustion processes. More specifically, it is believed to be one of the main reactions involved in the reduction of nitric oxide by reburning processes.[1] Being without barrier, this reaction is also involved in interstellar chemistry.[2] Therefore, many experiments have been carried out to determine its overall rate constant with a variety of techniques.[3−11] At 300 K, there is a general agreement for a rate constant about 1.9×10^{-10} cm^3 molecule^{-1} s^{-1}. No significant temperature dependence of the rate constant has been found over the range 13−3790 K,[1,4,6,9] except a slight increase at extremely low temperatures.[4] No pressure dependence of the rate constant could be detected in any of these experiments.[5] In contrast with the fact that its overall rate constant determination has been accurately determined over a wide range of temperature, very little is available about the product branching ratios, which are needed for the modeling of combustion or interstellar chemistry processes.

Owing to their exoergicities, chemical channels split themselves in different electronic pathways. The channel exothermicities are given hereafter with respect to ground-state products:

$$\mathbf{CH}(X^2\Pi) + \mathbf{NO}(X^2\Pi) \rightarrow \mathbf{CO}(X^1\Sigma^+) + \mathbf{NH}(X^3\Sigma^-, a^1\Delta, b^1\Sigma^+, A^3\Pi) \quad \Delta_r H^\circ_{298} = -4.62 \text{ eV} \quad (1)$$

$$\rightarrow \mathbf{H}(^2S) + \mathbf{NCO}(X^2\Pi, \tilde{A}^2\Sigma^+) \quad \Delta_r H^\circ_{298} = -3.22 \text{ eV} \quad (2)$$

$$\rightarrow \mathbf{O}(^3P, ^1D) + \mathbf{HCN}(X^1\Sigma^+) \quad \Delta_r H^\circ_{298} = -3.17 \text{ eV} \quad (3)$$

$$\rightarrow \mathbf{OH}(X^2\Pi) + \mathbf{CN}(X^2\Sigma^+, A^2\Pi_i) \quad \Delta_r H^\circ_{298} = -2.19 \text{ eV} \quad (4)$$

$$\rightarrow \mathbf{N}(^4S) + \mathbf{HCO}(X^2A', \tilde{A}^2A'') \quad \Delta_r H^\circ_{298} = -1.80 \text{ eV} \quad (5)$$

$$\rightarrow \mathbf{H}(^2S) + \mathbf{CNO}(X^2\Pi) \quad \Delta_r H^\circ_{298} = -0.61 \text{ eV} \quad (6)$$

The channels leading to O + HNC and N + HOC have not been included. Actually, the pathway leading to O + HNC is just less exoergic than that leading to O + HCN, so that the energy available to O + HNC is in large excess of the isomerization barrier of HNC into HCN. Most of HNC is thus expected to isomerize into HCN.[12] The N + HOC channel is less than 0.1 eV exoergic.[13] As shown below, it was found to be negligible by theoretical calculations[15] (0.1%). Finally, owing to the exoergicity of channel 5 and the easy dissociation of HCO through the predissociation of $\tilde{A}^2A''$, channel 5 should partially turn into

$$\mathbf{CH}(X^2\Pi) + \mathbf{NO}(X^2\Pi) \rightarrow \mathbf{N}(^4S) + \mathbf{H}(^2S) + \mathbf{CO}(X^1\Sigma^+) \quad \Delta_r H^\circ_{298} = -1.12 \text{ eV} \quad (7)$$

Okada et al.[5] probed the OH, CN, NH, and NCO products by laser-induced fluorescence, in a cell at room temperature, CH being obtained by the photolysis of $CHBr_3$ at 193 nm. On a kinetic basis, no conclusive evidence was presented. The product branching ratios of the channels yielding NH + CO and CN + OH were estimated to be 15% and 0.2%, respectively. The last one was determined by probing CN and not OH since the latter radical was also produced by the secondary reaction NH + NO. Dean et al.[1] studied the CH + NO reaction in a shock tube, over the temperature range 2600−3800 K. CH radicals were produced by the pyrolysis of CH_4 or C_2H_6. CN, N, O, OH, and NH radicals were probed by laser absorption or atomic resonance absorption spectroscopy (ARAS). The branching ratios were derived from kinetic simulations of experimental radical and atom profiles with various concentrations of precursors CH_4/NO or C_2H_6/NO. They estimated a contribution lower than 10% for CO + NH and lower than 30% for OH +

* Corresponding author: e-mail dorthe@cribx1.u-bordeaux.fr.; FAX (33) 556846645.

S1089-5639(98)02092-1 CCC: $15.00
Published on Web 09/29/1998

CN product channels. O + HCN was estimated to be the principal product channel but no percentage was proposed. Nishiyama et al.[7] determined the internal energy distribution of NH($A^3\Pi$) in a fast-flow reactor, the CH radical being produced by the C(^{1}D) + H_2 reaction. The populations of the vibrational levels $v' = 1$ and 0 were found to be 33% and 67%, respectively.

The most comprehensive experimental study of the branching ratios was not carried out on the CH + NO reaction itself but on the homologous CD + NO reaction by Lambrecht and Herschberger,[14] in a cell at 296 K. CD was produced by the photolysis of $CDBr_3$ at 266 nm. DCN, CO, CN, and DCO as direct products, and CO_2 and N_2O as products of subsequent reactions, were probed in one rovibrational state, using time-resolved infrared diode laser spectroscopy. The product branching ratios were calculated by assuming a Boltzmann distribution of vibrational states. To limit the contributions of the CD excited states produced by the photolysis of $CDBr_3$, a buffer gas (Xe) was thus introduced and the product branching ratios actually depended on the buffer gas pressure. After consideration of important secondary reactions, the following product branching ratios were obtained: O + DCN, (47.5 ± 12.2)%; D + NCO, (18.8 ± 5.5)%; OD + CN, <7.5%; and for the sum of the CO + ND and DCO + N channels, (33.7 ± 13.8)%. No mention of electronically excited products was reported. However, as shown by the theoretical study of Marchand et al.,[15] the CD + NO and CH + NO reactions do not present the same branching ratios for homologous pathways so that the experimental results of Lambrecht and Herschberger[14] for CD + NO cannot be transposed to CH + NO.

Using a RRK method, Bozzelli et al.[16] predicted an overall rate constant of 1.83×10^{-10} cm^3 molecule^{-1} s^{-1} at 300 K for the CH + NO reaction. They further proposed the following product branching ratios: O + HCN, 48%; N + HCO, 28%; H + NCO, 18%; CO + NH, 6%; and OH + CN, 5%. More recently, Marchand et al.[15] determined by ab initio calculations the topology of the lowest potential energy surface of triplet multiplicity involved in the reaction. The triplet surface is expected to play a major role in the reaction, because no barrier was found along the entrance channel, in contrast with the singlet surface. The rate constant, overall and detailed over the products, was calculated from this triplet surface by using a microcanonical approach of the transition state theory relying on the RRKM method. The overall rate constant was found to be 1.86×10^{-10} cm^3 molecule^{-1} s^{-1} at 300 K. The following branching ratios were reported: O + HCN, 72.4%; H + NCO, 13.9%; CO + NH, 8.2%; H + CNO, 3.3%; OH + CN, 1.4%; N + HCO, 0.6%; O + HNC, 0.1%; and N + HOC, 0.1%. The branching ratios were found to depend on isotopic effects and their values were also determined for CD + NO reaction: i.e., O + DCN, 53.8%; D + NCO, 24.0%; N + DCO and CO + ND, 20.3%; and OD + CN, 2.2% in fair agreement with the experimental results of Lambrecht and Herschberger.[14]

We performed the study of the CH + NO reaction in a low-pressure fast-flow reactor at room temperature. A clean source of CH radicals was provided by the reaction of potassium atoms with bromoform. The decay of CH probed by laser-induced fluorescence (LIF), NO being introduced in excess, allowed us to check the overall rate constant. However, our main interest was to improve, as far as possible, the product branching ratio determination. The product branching ratios over the channels yielding two diatomic species could not be determined as, owing to the exoergicities, many rovibronic levels were populated and only a few of them could be probed by laser-induced fluorescence. Under our experimental conditions, the thermalization was completed over rotational levels but not over vibrational levels and electronic states. The lack of vibronic thermalization prevented recovery of the relative concentrations of diatomic species from the probed levels. However, laser-induced fluorescence allowed us to check the occurrence of these pathways and chemiluminescence allowed some insight in the dynamics of radiative products. Actually, relative branching ratios could be determined for the reaction channels leading to a triatomic species and an atom, using the vacuum UV resonance fluorescence of the atom.

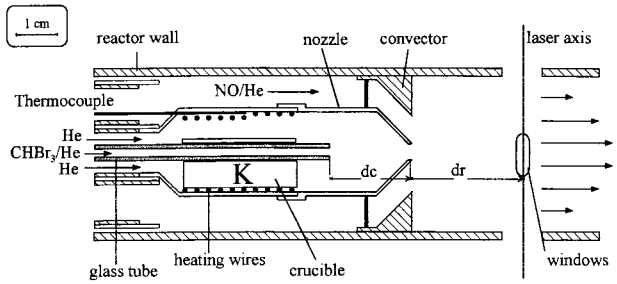

Figure 1. Reactant injector.

II. Experimental Section

A. Fast-Flow Reactor. The fast-flow reactor has been detailed elsewhere[17] and only a brief description is thus given. It consisted of a hollowed-out stainless steel block, with four perpendicular optical ports for detection by chemiluminescence and laser-induced fluorescence, in which a 36-mm inner diameter Teflon tube was inserted. The reactant injector, sliding along the Teflon inner wall of the reactor, has been slightly modified (Figure 1). In its first version,[17] pieces of potassium were stored in a cylindrical fine mesh sleeve around the central glass tube. However, according to the temperature and the He flow, it happened that melting potassium was pouring out from the mesh, shortening the time available for the experiments. A crucible thus replaced the fine mesh sleeve. The distance (dr) between the window detection and the injector nozzle aperture could vary over the range 0−100 mm with 0.5-mm precision. The reactor was pumped by a Roots blower (Edwards EH 500) backed by a two-stage mechanical pump (Edwards E2M80). Before each experiment, the vacuum and the leak-plus-outgassing rate were checked with a Pirani gauge (respectively <0.05 mTorr and <10 mTorr min^{-1}). A 10.6 mm diameter diaphragm at the inlet of the Roots blower gave a flow velocity of 26.5 m s^{-1} for a total pressure of 2.0 Torr, the buffer gas being He with a purity ≥99.995%. The pressure was measured by a capacitance manometer (Barocel 0−10 Torr) and the flow rates were adjusted by thermal mass flow meters (Tylan).

CH, CHBr, and CN radicals were probed by laser-induced fluorescence (LIF) with a Nd−YAG laser (Quantel YG 581C) pumped dye laser. Excitation was about 431 nm (coumarin 440), 590 nm (rhodamine 610), and 388 nm (second H_2 Raman anti-Stokes radiation with rhodamine 560), respectively. Fluorescence from the reactor center was imaged, through two plan-convex lenses enclosing an appropriate combination of filters, onto the photocathode of a Hamamatsu R106 photomultiplier tube. For the CH ($A^2\Delta \leftarrow X^2\Pi$, $\Delta v = 0$) excitation, fluorescence over the $\Delta v = -1$ sequence was detected through an interference filter centered at 480.0 nm and color-glass filters (MTO J495). The fluorescence above 600 nm following the CHBr ($\tilde{A}^1A'' \leftarrow X^1A'$, 2^7_0) excitation[18] was collected with 3 color-glass filters (MTO 603, 610, and 660). The $\Delta v = -1$

CN fluorescence following the ($B^2\Sigma^+ \leftarrow X^2\Sigma^+$, $\Delta v = 0$) excitation was selected with an interference filter centered at 415 nm and a color-glass filter (MTO J423a). The signal monitored by an oscilloscope (Tektronix 2440) was transferred to a microcomputer.

The chemiluminescence signal from the reaction zone was collected by a quartz lens and dispersed over the 195−850 nm wavelength range by a Jobin-Yvon HRS2 monochromator using a 1200 grooves/mm grating blazed at 500 nm (3M210R) or 253.6 nm (2M210R). A homemade automatic scanner and numeric digitizer controlled the monochromator and stored the Hamamatsu 955 photomultiplier signal, which was transferred to a microcomputer.

B. Clean Source of CH Radicals. CH radicals were produced in the reactant injector nozzle from the $CHBr_3 + 3K \rightarrow CH + 3KBr$ overall reaction (Figure 1), which can be separated into the elementary steps:

$$CHBr_3 + K \rightarrow CHBr_2 + KBr \qquad \Delta_r H^\circ_{298} = -1.02 \pm 0.09 \text{ eV}^{19} \quad (8)$$

$$CHBr_2 + K \rightarrow CHBr + KBr \qquad \Delta_r H^\circ_{298} = -0.77 \pm 0.1 \text{ eV}^{19} \quad (9)$$

$$CHBr + K \rightarrow CH + KBr \qquad \Delta_r H^\circ_{298} = -0.38 \pm 0.2 \text{ eV}^{19} \quad (10)$$

As all the $K + CHBr_x \rightarrow KH + CBr_x$ ($x \geq 0$) reactions are endoergic, this source can only produce CH. According to Anderson et al.,[20] who also used such a source for CH radicals, the first step could have a rate constant around 3×10^{-10} cm^3 molecule^{-1} s^{-1}. The main reactions removing CH should be CH + CHBr with a rate constant[20] of $\approx 10^{-10}$ cm^3 molecule^{-1} s^{-1} and CH + CH with an overall rate constant of 2.5×10^{-10} cm^3 molecule^{-1} s^{-1} as estimated by Dean et al.[21] To minimize the CH + CHBr reaction, we adjusted the microfurnace temperature and the bromoform flow introduced by the glass tube (Figure 1) in order to get an excess of potassium atoms in the nozzle ([K] > 20[$CHBr_3$]). Under our conditions, the principal secondary (and unavoidable) reaction thus was CH + CH.

To optimize the CH production, the CH and CHBr radicals were probed by LIF when varying the different parameters such as the oven temperature, the $CHBr_3$ flow, and the carrier-gas flows. The variation of the LIF signals versus the distance between the end of the glass tube and the nozzle aperture (thus determining the reaction time for given reactant flows and total pressure) is represented in Figure 2. In the simulation of the CH and CHBr evolutions, the $CHBr_3$ + K rate constant was fixed at 3×10^{-10} cm^3 molecule^{-1} s^{-1} and that of the CH + CH reaction at 2.5×10^{-10} cm^3 molecule^{-1} s^{-1}. The rate constant of the second and the third bromine atom strippings are approximately (0.9 ± 0.5) and $(3 \pm 2.5) \times 10^{-10}$ cm^3 molecule^{-1} s^{-1}, respectively, in the plug-flow approximation and supposing a constant temperature in the nozzle. As already stated, the major CH radical losses came from the CH + CH reaction (which leads to $C_2H + H$ and $C_2 + H_2$)[22] and from the wall.

The overall rate constant determination of the CH + NO reaction was performed with a low $CHBr_3$ flow and with the maximum distance between the end of the glass tube and the nozzle aperture. Under these conditions, the CH production was small but we were sure to get in the reactor only CH radicals, K atoms, KBr molecules, and a negligible CH + CH reaction rate with respect to that of CH + NO. The CH

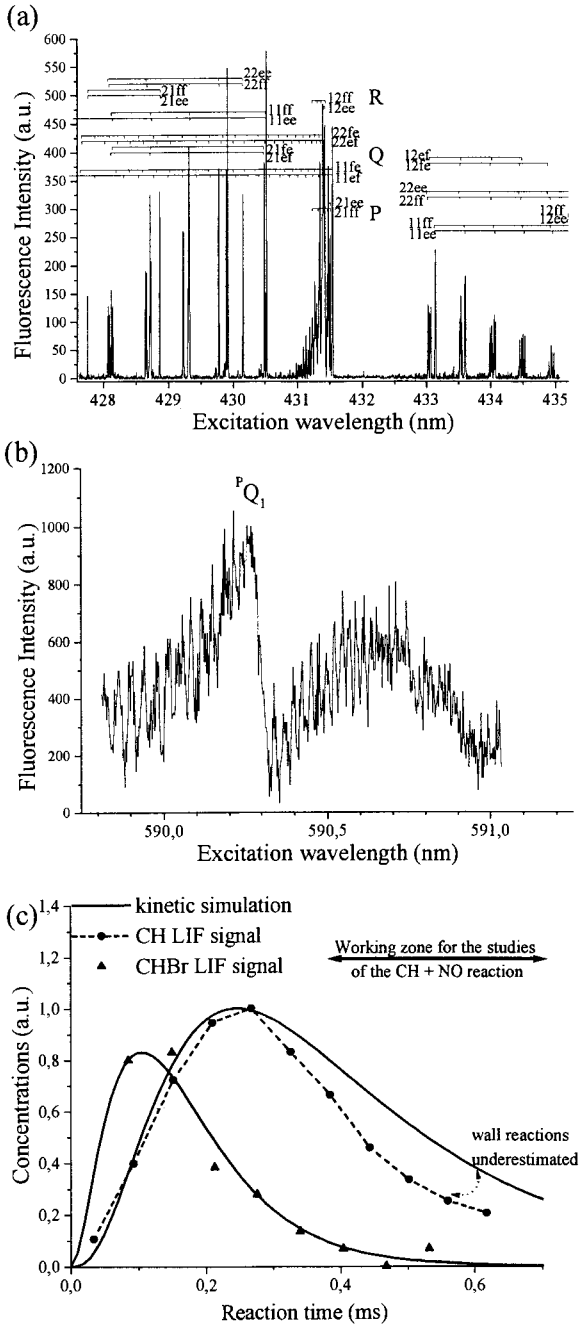

Figure 2. (a) CH excitation spectrum. (b) CHBr excitation spectrum. (c) Experimental fluorescence intensity evolutions of CH and CHBr and kinetic simulation.

excitation spectrum showed that CH was produced only in the vibrational level $v = 0$ of the ground electronic state. As the detection of atomic products given by CH + NO reaction required a CH concentration higher than that used for the overall rate constant determination, the CH + CH reaction could not be neglected in the experiments devoted to the product branching ratios. The influence of the latter reaction was thus systematically studied.[22] The NO radical (99.90%, Air Liquide) was used directly from the cylinder without further purification.

C. Atom Detection. As atom concentrations in the reactor were too low for absorption measurements, N, H, and O atoms were probed by their resonance fluorescence at 120.00, 121.57, and 130.35 nm, respectively. Excitation of all these atoms was achieved, at the same time, with a microwave discharge lamp giving atomic emission lines on these transitions and powered at 125 W and 2450 MHz (EMS, Microtron 200 microwave

generator). It consisted of a Vidal cavity[23] mounted on a quartz tube isolated from the reactor by a biconvex LiF lens and pumped by a mechanical pump (Alcatel M2012). Atomic emission from the lamp and fluorescence from atomic products were collected through MgF_2 windows and a LiF biconvex lens onto a ARC VM502 monochromator with a 1200 grooves/mm Al + MgF_2 grating blazed at 120 nm and a Hamamatsu R1459 solar-blind photomultiplier tube. After amplification, the signal was sent to the oscilloscope used as a voltmeter. The vacuum of this vacuum UV monochromator was kept below 10^{-5} mbar by a turbomolecular pump (Turbovac 50, Leybold) backed by a mechanical pump (Trivac D1,6B, Leybold). The direct focus of the lamp emission and that of the fluorescence onto the monochromator required a change in the position of the lamp from a port along the axis of the monochromator to a port at right angles. This change in the lamp position required 2−3 h to achieve stabilization at the second switching on. To avoid it, the lamp was always kept in the perpendicular position needed for fluorescence detection. The atomic excitation line intensities of the lamp were checked at the beginning and at the end of each experiment by the scattering at right angles of the lamp emission on the central glass tube, which was used to inject the halomethane and was moved forward to allow this scattering. The spectral distributions of the line intensities of the lamp recorded either directly or by scattering on the glass tube were identical. The pressure in the quartz tube of the lamp was typically 2 Torr and the flow was 40 standard cubic centimeters per minute (sccm). The flow consisted of He (AirGaz 99.9995% purity) carrying a known premixed $N_2/H_2/O_2$ mixture to get optimal emission intensities from excited N, H, and O atoms. The relative concentrations in the lamp were typically 12 ppm H_2, 6 ppm N_2, and 61 ppm O_2. To obtain the relative atomic concentrations in the reactor, the fluorescence signal was divided by the lamp emission intensity. However, to ensure the linear dependence of the atomic fluorescence versus the lamp emission intensity, the atomic concentration in the reactor being constant, the multiplet emission intensities had to be known as well as the extent of the line self-reversal in the lamp. As our monochromator could not resolve the fine structure of atomic lines, the sublevel electronic populations of the excited atoms in the lamp were supposed to be proportional to their statistical weights[24] (this hypothesis has been verified with the carbon: the ratios of fluorescence and lamp emission have been measured on the three electronic transitions at 132.9, 156.0, and 165.7 nm,[25] C atoms being obtained with the CBr_4 + 4K system). To verify that the lamp emission atomic lines were nonreversed (for N, H, and O), we used the following procedure. The ratios of the atomic fluorescence versus the emission lamp intensity were measured by varying the calibrated mixture flow in the He main flow in the lamp while the atomic concentration in the reactor was kept constant. For the H line at 121.6 nm, for example, this ratio was constant as long as the H_2 lamp concentration was lower than 8 ppm (at 2 Torr of He) and then decreased (the lamp emission is never zero since impurities are always present even with He alone). This behavior is due to the fact that the measured emission intensity is integrated over the whole line profile whereas the fluorescence intensity is the convolution of the absorption and emission profiles. When the line is reversed, the lamp emission line profile is larger than that with just a Doppler broadening and presents a hollow at the line center, the overall intensity being constant. It resulted that the atomic absorption in the reactor was less efficient and the fluorescence was not proportional to the lamp emission intensity. The conditions for which the emission line profiles were not reversed were determined from a simulation of the lamp emission with a two-layer model[26] (an emitting plus absorbing zone, the discharge plasma, and an absorbing zone directly in front of the discharge). Moreover, as the atomic concentration in the reactor itself was very low (the measured Lyman-α absorption was on the order of a few percent), the fluorescence intensity divided by the lamp emission intensity was proportional to the atomic concentration for all the electronic transitions.[25] The emission lamp was carefully measured at the beginning and at the end of each day and the lamp quartz tube was filled with a static pressure of He when the experiments were over. The lamp emission remained quite constant over several days.

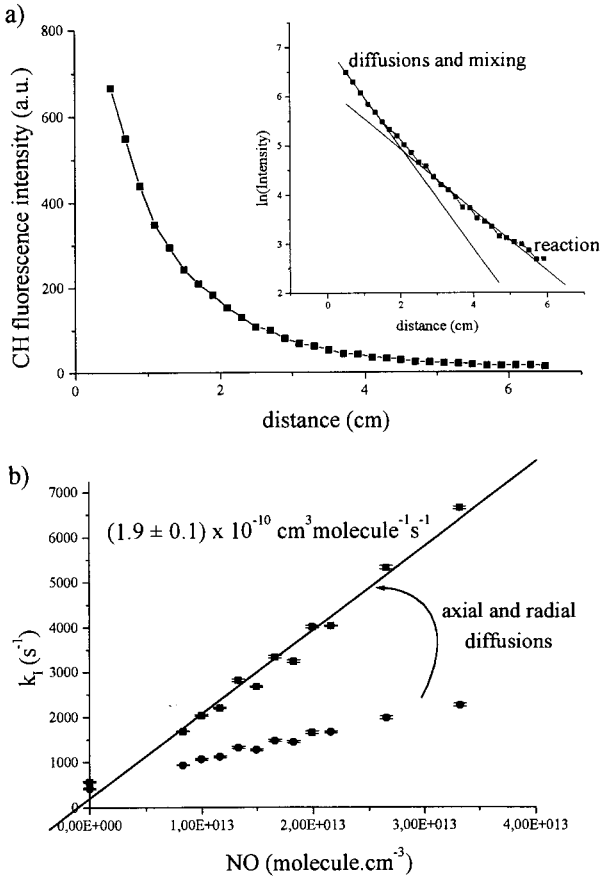

Figure 3. Determination of the CH + NO overall rate constant. (a) Example of CH decay for [NO] = 2.657×10^{13} molecule cm^{-3}. (b) Plot of pseudo-first-order rate constants corrected from axial and radial diffusions.

III. Results

A. Overall Rate Constant of the CH + NO Reaction. The CH + NO overall rate constant was determined from the CH LIF signal decay observed with NO in large excess of CH (Figure 3). However, in its early stages, the decay of the observed CH signal resulted mainly from the lowering of CH density by the diffusion needed to fill a cross section of the reactor after the nozzle exit. As NO had also to diffuse to fill a cross section of the reactor, the CH + NO reaction itself was delayed by mixing effects. A convector, immediately downstream of the nozzle, reduced the mixing time significantly (Figure 1). To get rid of the mixing effects, only the last stages of the decay have been taken to determine the pseudo-first-order rate constant. The measured rate constant did not vary linearly with the NO concentration, rate constant values at large

NO concentrations being smaller than those expected from a linear extrapolation of values obtained at low NO concentrations. This deviation stems from the diffusion induced by the large radial and axial concentration gradients occurring because the CH + NO reaction is very fast. To correct for these diffusion effects, the formula of Keyser[27] was used:

$$k_{cor} = k_{obs}\left[1 + \left(\frac{d^2}{48D} + \frac{D}{v^2}\right)k_{obs}\right]$$

where k_{obs} is the observed first-order rate constant, d is the diameter of the reactor, and v is the average flow velocity. The diffusion coefficient D of CH in He was determined from that of OH given by Keyser[27] (730 Torr cm^2 s^{-1} at 295 K) multiplied by $[M_{OH}/M_{CH}]^{1/2}$ (to account for the difference in molecular weight) and with a temperature dependence of $T^{1.5}$.

The corrected value of the pseudo-first-order rate constant varied linearly with the NO concentration, which gives an overall rate constant of $(1.9 \pm 0.5) \times 10^{-10}$ cm^3 molecule^{-1} s^{-1}. This value agrees quite well with the recently reported experimental values in a cell[3,4,6,9,10] and with the theoretical value $(1.86 \pm 0.3) \times 10^{-10}$ cm^3 molecule^{-1} s^{-1} calculated by Marchand et al.[15]

B. Diatom and Diatom Products. The chemical channels split into two classes, those that lead to two diatomic species and those that lead to an atom and a triatomic species. Relative branching ratios from laser-induced fluorescence experiments on diatomic or triatomic species can be determined only if a nearly complete thermalization over rotational, vibrational, and electronic levels occurs, since in such a case it can be possible to relate the density of probed levels to that of the species through the Maxwell−Boltzmann relationship. Owing to the exoergicities of the reaction pathways, products are rotationally, vibrationally, and electronically excited. Under our He pressure, relaxation over rotational levels of the products was complete but not that over vibrational levels and electronic states. This aspect was previously found for the vibrational distribution of CN produced by the N + C_2 reaction under the same experimental conditions.[17] The relative diatomic product densities could thus not be determined from LIF experiments. Nevertheless, some information could be obtained for pathways leading to diatomic species. For example, the exoergicity of the pathway leading to CN + OH allows the production of the CN radical in its first radiative electronic state $A^2\Pi_i$. We could not detect the chemiluminescence in the visible on the CN-($A^2\Pi_i \rightarrow X^2\Sigma^+$) transition. Also, we could not find CN by LIF on the ($B^2\Sigma^+ \leftarrow X^2\Sigma^+$) transition, while we probed it quite easily when produced by the N + $C_2 \rightarrow$ CN + C and N + CH $\rightarrow$ CN + H reactions,[17] for which reactants densities were much lower than for the CH + NO reaction. This suggests that the pathway leading to CN + OH is negligible. Actually, we observed a weak CN ultraviolet chemiluminescence from the CN($B^2\Sigma^+ \rightarrow X^2\Sigma^+$) transition. The exoergicity of the channel yielding CN + OH does not allow the production of CN($B^2\Sigma^+$). This chemiluminescence arose from the strongly exoergic C_2 + NO $\rightarrow$ CN + CO reaction,[28] C_2 being a minor product of the CH + CH reaction in the nozzle.

Among the three excited electronic states of the NH radical that can be populated, according to the exoergicity of the pathway leading to CO + NH, only NH($A^3\Pi$) has been detected from the chemiluminescence of the ($A^3\Pi \rightarrow X^3\Sigma^-$, $\Delta v = 0$) transition at about 337 nm (Figure 4). NH($A^3\Pi$) was populated up to $v' = 2$, which lies 0.20 eV below the NH energy limit defined by the total energy available to the products of the

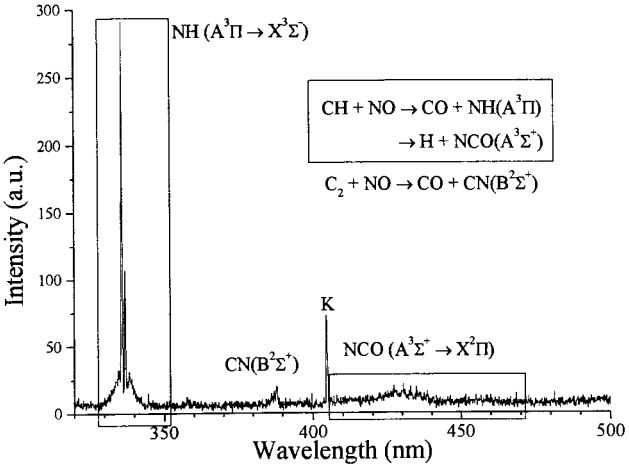

Figure 4. CH + NO chemiluminescences at a total pressure of 1.6 Torr.

pathway involved; the $v' = 3$ level is above this energy limit. The NH chemiluminescence signal was proportional to the CH LIF signal whatever the $CHBr_3$ concentration. The kinetic studies performed with the NH($A^3\Pi$) chemiluminescence signal led to the same overall reaction rate constant for CH + NO as that obtained from the LIF CH decay. Thus NH($A^3\Pi$) is directly produced by CH + NO. We also observed that the detection of diffusion or mixture problems was easier from the NH chemiluminescence decay than from the LIF CH decay. The chemiluminescence signal of the $\Delta v = 0$ transition did not exhibited pressure dependence over the limited pressure range 1−3 Torr. The branching ratio of the channels leading to CO + NH($A^3\Pi$, $v' = 1$) and CO + NH($A^3\Pi$, $v' = 0$) was estimated. As NO is in excess, the NH radical reacts essentially only with it. However, the NH + NO reaction[29] and the quenching[30] pseudo-first-order rate constants are negligible compared with the emission rate constant ($1/\tau_{v'}$) since the two vibrational levels lifetimes ($\tau_{v'}$) are very short ($\tau_0 = 440 \pm 15$ ns and $\tau_1 = 420 \pm 35$ ns).[30] Applying the steady-state approximation to excited NH, the relation between the rate constant for the production of vibrational levels and their concentration is obtained:

$$\frac{d[NH(A^3\Pi, v')]}{dt} \approx 0 = k_{v'}[CH][NO] - \frac{1}{\tau_{v'}}[NH(A^3\Pi, v')]$$

The ratio of chemiluminescence intensities, determined from the area of vibronic bands, is related to the ratio of rate constants for vibrational level production through

$$\frac{S(v'=1)}{S(v'=0)} = \frac{A_{11}[NH(A^3\Pi,1)]\bar{v}_{11}}{A_{00}[NH(A^3\Pi,0)]\bar{v}_{00}} = \frac{A_{11}\tau_1\lambda_{00}k_{v'=1}}{A_{00}\tau_0\lambda_{11}k_{v'=0}}$$

where $A_{00} = 0.2522 \times 10^{-7}$ s^{-1} and $A_{11} = 0.2169 \times 10^{-7}$ s^{-1} are the Einstein coefficients calculated by D. Yarkony,[29] and $\lambda_{00} = 334.85$ nm and $\lambda_{11} = 335.9$ nm are the Q branch wavelengths for both transitions.

The following branching ratio has been found:

$$\frac{k_{NH(A^3\Pi,v'=1)}}{k_{NH(A^3\Pi,v'=0)}} = 0.49 \pm 0.03 = \frac{(33 \pm 3)\%}{(67 \pm 3)\%}$$

in excellent agreement with Nishiyama et al.[7] They determined the internal energy distribution of NH($A^3\Pi$) in a reactor where CH radicals were produced by the C(^{1}D) + H_2 reaction, the

excited carbon atoms being obtained by a discharge through a CO/He mixture.

The OH chemiluminescence given by the CH + O_2 → CO + OH reaction is often used as a tracer of the CH radical. Experiments with a mixture of O_2/NO have been performed to compare the chemiluminescence signals from CH + O_2 and CH + NO. The branching rate that leads to excited OH formation from the CH + O_2 reaction is 20 times higher than that for excited NH from CH + NO. If the branching ratio of the channel CH + O_2 → OH* + CO is 0.48%, as estimated by Grebe et al.,[31] the product branching ratio of CH + NO → NH* + CO is less than 0.02%.

C. Atom + Triatom Products. *1. Chemiluminescence.* The CH + NO reaction can produce NCO and HCO in their excited electronic states. However, since HCO in its first electronic state is predissociative, it cannot be detected. The chemiluminescence of NCO was readily detected but the strong overlapping of vibronic bands did not allow determination of the internal energy distribution. The chemiluminescence signal exhibits the same behavior as that of NH, against the $CHBr_3$ concentration or the distance. The NCO radical thus was directly produced by the CH + NO reaction. The relative product branching ratios of the channels yielding NH* + CO and NCO* + H were estimated by integrating the total chemiluminescence signal of the two radicals. The same approximations as in the NH study were made. NCO reacts essentially with NO with a rate constant of 3.4×10^{-11} cm^3 $molecule^{-1}$ s^{-1}.[32] The rate constants of the chemical reaction of excited NCO and of its collisional quenching with NO are unknown. Nevertheless, even with a gas kinetic value, owing to the NO concentration, the corresponding pseudo-first-order rate constant should be about 10^4 s^{-1}, while the spontaneous emission rate constant is 3×10^6 s^{-1}.[33] With Ar, no pressure dependence of the radiative lifetime[33] could be detected over the range 0.5−4.0 Torr. It is thus also expected with He. With these approximations, the result is

$$\frac{k_{CH+NO\rightarrow H+NCO^*}}{k_{CH+NO\rightarrow CO+NH^*}} = 1.4 \pm 0.1 = \frac{(58 \pm 7)\%}{(42 \pm 7)\%}$$

2. Branching Ratios. To determine the product branching ratios over the channels yielding an atom and a triatomic molecule, the atomic fluorescence was used. First, it was checked that the atomic absorption was small. In this condition, the fluorescence signal divided by the emission intensity is proportional to $f_A/\delta_A[A]$, [A] being the atomic concentration, f_A the oscillator strength,[25] and δ_A the Doppler broadening (T = 300 K).[26] A typical atomic fluorescence spectrum is shown in Figure 5.

The two sources of error in the atomic branching determination could be an underestimation of N atoms due to their removal by N + NO → N_2 + O and an overestimation of H atoms due to the contribution of the CH + CH → C_2H + H reaction. Nitrogen atoms react with NO at room temperature with a rate constant of $(2.9 \pm 1.0) \times 10^{-11}$ cm^3 $molecule^{-1}$ s^{-1},[32] 7 times lower than the CH + NO rate constant. A kinetic simulation with and without removal of N atoms by NO has confirmed a negligible reduction of N atom density by the N + NO reaction over the reaction time spanned for atom probing, i.e., at the beginning of the CH + NO reaction. So, the major source of error in the atomic branching determination could be the CH + CH reaction. With no NO added, the H atom fluorescence started from zero at the exit of the nozzle (Figure 5c), which means that nearly all the H atoms produced by the CH + CH reaction in the nozzle were removed by the metallic wall of the nozzle. The H atoms from CH + CH were thus produced in the reactor itself. When a large excess of NO was introduced, this secondary reaction CH + CH was minimized. Over the first millisecond of reaction time, the ratios between N, H, and O atom densities did not change, confirming the negligible contribution of the CH + CH reaction when NO is in excess. The ratios were also kept constant when the $CHBr_3$ concentration was changed. The relative atom branching ratios were 4−10% N, 20−30% H, and 60−80% of O.

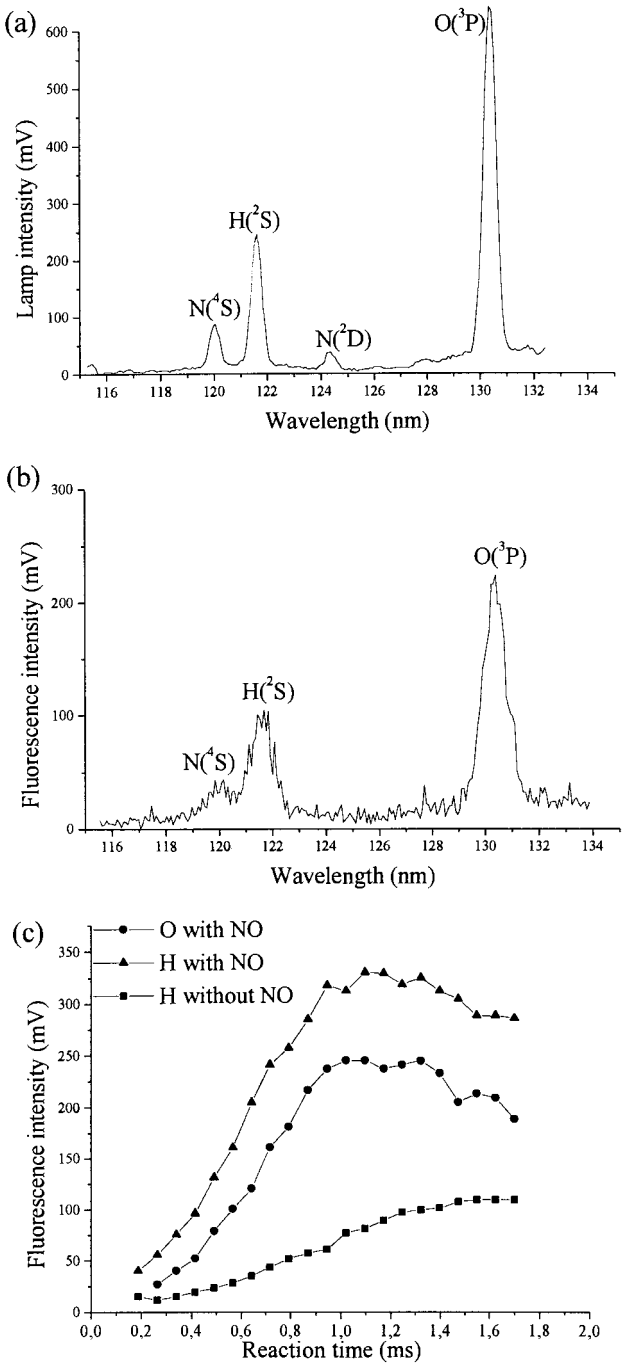

Figure 5. (a) Atomic emission spectrum of the resonance lamp. (b) Atomic resonance fluorescence during the CH + NO reaction study (scattered light of the lamp emission was less than 5 mV). (c) H and O atom fluorescence with [NO] = 3.4×10^{13} molecule cm^{-3}. Without NO, fluorescence from H was produced by CH + CH → C_2H + H.

IV. Discussion

As the energy available to N + HCO is 1.12 eV above the

TABLE 1: CH + NO Product Branching Ratios

channel	our results flow reactor	Marchand[15] theory	Dean[1] shock tube	Okada[5] cell	
O	(72 ± 10)%	80.2%			sum over atom
H	(21 ± 10)%	19.0%			branching ratios
N	(7 ± 3)%	0.8%			= 100%
O + H + N	major	90.4%	major	major	sum over all
NH + CO	?	8.2%	<10%	15%	branching ratios
CN + OH	negligible	1.4%	<30%	≈0.2%	= 100%

TABLE 2: CD + NO Product Branching Ratios

channel	Marchand[15] theory	Lambrecht[14] cell
O + DCN	53.8%	(47.5 ± 12)%
D + NCO	24.0%	(18.8 ± 5.5)%
ND + CO and N + DCO	20.0%	(33.7 ± 13.8)%
CN + OD	2.2%	<7.5%

HCO dissociation energy, the HCO radical is likely to be partially decomposed into H + CO. Thus, the measured H atom concentration comes both from the H + NCO and N + H + CO channels. This possibility is taken into account in the results displayed in Table 1. Branching ratios calculated by Marchand et al.[15] are the following: O + HCN, 72.4%; O + HNC, 0.1%; H + NCO, 13.9%; H + CNO, 3.3%; CO + NH, 8.2%; OH + CN, 1.4%; N + HCO, 0.6%; and N + HOC, 0.1%. To compare with our results, the calculated branching ratios over the channel yielding an atom and a triatomic isomer were transformed and arranged with respect to atomic products, with a sum equal to 100% (Table 1). There is good agreement between experiment and theory for O and H atoms but not for N atoms, which seem to be clearly underestimated in the theoretical calculations. The calculated contribution[15] of pathways leading to N atoms is lower than that of the pathway leading to CN + OH; by contrast, the detection sensitivity of CN allowed us to ascertain that the pathway leading to CN + OH is negligible, even with respect to pathways leading to N atoms. It was thus interesting to compare the CD + NO reaction branching ratios calculated with the same potential energy surface to the experimental results of Lambrecht and Herschberger[14] (Table 2). Our experimental data for CH + NO and those of Lambrecht and Herschberger[14] for CD + NO agree with the theoretical studies,[15] except for the N + HCO and N + DCO pathways, which appear to be underestimated by theoretical calculations. This difference could come from a possible missing direct decomposition channel of the OC(N)H intermediate into OCH + N product channel in the topology of the potential energy surface[15] and also, but less clearly, from the possible contribution of the singlet surface, which was not taken into account.

The theoretical results give a complete distribution of the branching ratios over all the exoergic pathways while the experiments can give the distribution over only some of them. The good agreement between our experimental results on the CH + NO reactions and those of Lambrecht and Herschberger[14] on CD + NO with the theoretical calculations carried out by Marchand et al.[15] establishes confidence in the theoretical branching ratios, except for an underestimation of the pathways leading to N atoms, which thus results in a slight overestimation of the others. Combining our experimental results with the calculated[15] results, we anticipate that the actual distribution should not be very far from the following: O + HCN, 69%; H + NCO, 13%; CO + NH, 8%; N + (HCO and H + CO), 6%; H + CNO, 3% and CN + OH, 1%.

Acknowledgment. This work was supported by the European Community through the HCM network Multichannel Reactions and Kinetic Modeling (Contract ERBCHRCT940436) as well as by the CNRS through the Groupement de Recherche Physico-Chimie des Molécules et Grains Interstellaires.

References and Notes

(1) Dean, A. J.; Hanson, R. K.; Bowman, C. T. *J. Phys. Chem.* **1991**, *95*, 3180.

(2) (a) Lindqvist, M.; Sandqvist, Aa.; Winnberg, A.; Johansson, L. E. B.; Nyman, L.-Å. *Astron. Astrophys. Suppl. Ser.* **1995**, *113*, 257. (b) Rieu, N.-Q.; Henkel, C.; Jackson, J. M.; Mauersberger, R. *Astron. Astrophys.* **1991**, *241*, 233.

(3) Mehlmann, C.; Frost, M. J.; Heard, D. E.; Orr, B. J.; Nelson, P. F. *J. Chem. Soc., Faraday. Trans.* **1996**, *92*, 2335.

(4) Bocherel, P.; Herbert, L. B.; Rowe, B. R.; Sims, I. R.; Smith, I. W. M.; Travers, D. *J. Phys. Chem.* **1996**, *100*, 3063.

(5) Okada, S.; Yamasaki, K.; Matsui, H.; Saito, K.; Okada, K. *Bull. Chem. Soc. Jpn.* **1993**, *66*, 1004.

(6) Becker, K. H.; Engelhardt, B.; Geiger, H.; Kurtenbach, R.; Wiesen, P. *Chem. Phys. Lett.* **1993**, *210*, 135.

(7) Nishiyama, N.; Sekiya, H.; Yamaguchi, S.; Tsuji, M.; Nishimura, Y. *J. Phys. Chem*. **1986**, *90*, 1491.

(8) Lichtin, D. A.; Berman, M. R.; Lin, M. C. *Chem. Phys. Lett.* **1984**, *108*, 18.

(9) Berman, M. R.; Fleming, J. W.; Harvey, A. B.; Lin, M. C. *Chem. Phys.* **1982**, *73*, 27.

(10) Wagal, S. S.; Carrington, T.; Filseth, S. V.; Sadowski, C. M. *Chem. Phys.* **1982**, *69*, 61.

(11) Butler, J. E.; Fleming, J. W.; Goss, L. P.; Lin, M. C. *Chem. Phys.* **1981**, *56*, 355.

(12) (a) Bentley, J. A.; Bowman, J. M.; Gazdy, B.; Lee, T.; Dateo, C. *Chem. Phys. Lett.* **1992**, *198*, 563. (b) Lee, T. J.; Rendell, A. P. *Chem. Phys. Lett*. **1991**, *177*, 491.

(13) (a) Bowman, J. M.; Bittman, J. S.; Harding, L. B. *J. Chem. Phys.* **1986**, *85*, 911. (b) Geiger, L. C.; Schatz, G. C.; Harding, L. B. *Chem. Phys. Lett.* **1985**, *114*, 520.

(14) Lambrecht, R. K.; Hershberger, J. F. *J. Phys. Chem.* **1994**, *98*, 8406.

(15) (a) Marchand, N.; Jimeno, P.; Rayez, J.-C.; Liotard, D. *J. Phys. Chem. A* **1997**, *101*, 6077. (b) Marchand, N.; Rayez, J.-C.; Smith, S. C. *J. Phys. Chem. A* **1998**, *102*, 3358. Note: Our colleagues have mistaken in citing, in their own references, the present article as "in press in *Chem. Phys.*" while it was still in preparation and was never submitted to *Chem. Phys.*

(16) Bozzelli, J. W.; Dean, A. M.; *Combustion Chemistry of Nitrogen Compounds: A Comprehensive Review and Analysis of Selected Reactions*, 2nd ed.; W.C. Gardiner, in press.

(17) (a) Daugey, N.; Bergeat, A.; Schuck, A.; Caubet, P.; Dorthe, G. *Chem. Phys.* **1997**, *222*, 87. (b) Daugey, N.; Bergeat, A.; Caubet, P.; Cecarrelli, E.; Schuck, A.; Dorthe, G. *News Lett. Anal. Astron. Spec*. **1995,** *22*, 10.

(18) Xu, S.; Beran, K. A.; Harmony, M. D. *J. Phys. Chem.* **1994**, *98*, 2742.

(19) (a) Born, M.; Ingemann, S.; Nibbering N. M. M. *J. Am. Chem. Soc.* **1994**, *116*, 7210. (b) Tschuikow-Roux, E.; Paddison, S. *Int. J. Chem. Kinet.* **1987**, *19*, 15.

(20) Anderson, S. M.; Freedman, A.; Kolb, C. E. *J. Phys. Chem.* **1987**, *91*, 6272.

(21) Dean, A. J.; Hanson, R. K.; Bowman, C. T. *Twenty-third Symposium (International) on Combustion*; The Combustion Institute: Pittsburgh, PA, 1990; p 259.

(22) Bergeat, A.; Calvo, T.; Loison, J.-C.; Dorthe, G. Manuscript in preparation.

(23) Vidal, B.; Dupret, C. *J. Phys. E.: Sci. Instr*. **1976**, *9*, 998.

(24) Lin, C.-L.; Parkes, D. A.; Kaufman, F. *J. Chem. Phys.* **1970**, *53*, 3896.

(25) Wiese, W. L.; Fuhr, J. R.; Deters, T. M. *J. Phys. Chem. Ref. Data*, **1996**, *Monogr. 7*.

(26) Lynch, K. P.; Schwab, T. C.; Michael, J. V. *Int. J. Chem. Kinet.* **1976**, *8*, 651.

(27) Keyser, L. F. *J. Phys. Chem.* **1984**, *88*, 4750.

(28) Reisler, H.; Mangir, M. S.; Wittig, C. *J. Chem. Phys.* **1979**, *71*, 2109.

(29) Yarkony, D. R. *J. Chem. Phys.* **1989**, *91*, 4745.

(30) Fairchild, P. W.; Smith, G. P.; Crosley, D. R.; Jeffries, J. B. *Chem. Phys. Lett.* **1984**, *107*, 181.

(31) Grebe, J.; Homann, K. H. *Ber. Bunsen-Ges. Phys. Chem.* **1982**, *86*, 587.

(32) Baulch, D. L.; Cobos, C. J.; Cox, R. A.; Frank, P.; Hayman, G.; Just, Th.; Kerr, J. A.; Murrells, T.; Pilling, M. J.; Troe, J.; Walker, R. W.; Warnatz, J. *J. Phys. Chem. Ref. Data* **1994,** *23*, 847.

(33) Charlton, T. R.; Okamura, T.; Thrush, B. A. *Chem. Phys. Lett.* **1982**, *89*, 98.